

# Ownership Protection of Generative Adversarial Networks

Hailong Hu

SnT, University of Luxembourg

Jun Pang

FSTM & SnT, University of Luxembourg

## Abstract

*Generative adversarial networks (GANs) have shown remarkable success in image synthesis, making GAN models themselves commercially valuable to legitimate model owners. Therefore, it is critical to technically protect the intellectual property of GANs. Prior works need to tamper with the training set or training process, and they are not robust to emerging model extraction attacks. In this paper, we propose a new ownership protection method based on the common characteristics of a target model and its stolen models. Our method can be directly applicable to all well-trained GANs as it does not require retraining target models. Extensive experimental results show that our new method can achieve the best protection performance, compared to the state-of-the-art methods. Finally, we demonstrate the effectiveness of our method with respect to the number of generations of model extraction attacks, the number of generated samples, different datasets, as well as adaptive attacks.*

## 1. Introduction

Generative adversarial networks (GANs), as one of the most successful generative models, have already exerted revolutionary influences on many application domains, such as image synthesis [3, 10, 17, 25, 28], image editing [5, 31, 36, 44], and image translation [14, 22, 37, 45]. However, building a well-trained state-of-the-art GAN model is not straightforward. It usually requires the complicated and exhausting process of data collection, expert-level knowledge in model architecture design, elaborate hyperparameter tuning, and extensive computing resources. Therefore, a high-quality GAN model is incredibly costly and should be regarded as the intellectual property of the model owner.

As GAN models are valuable, this simultaneously incentivizes adversaries to steal these models in various ways. On the one hand, adversaries can physically steal a GAN model via malware infection or insider attacks [29]. An insider attack can directly copy the victim model through those who are authorized to access the full model. As a result, the stolen model is totally the same as the victim model. On the other hand, adversaries can functionally steal a GAN model

via model extraction attacks [13]. This threat exists because an increasing number of technology companies provide Machine Learning as a Service (MLaaS) to their customers, such as Amazon AWS, Google Cloud, and Microsoft Azure. A model extraction attack enables adversaries to obtain a substitute model via exposed interfaces. As a consequence, the stolen model is functionally similar to the victim model. In general, both physical stealing attacks and model extraction attacks seriously jeopardize the intellectual property of legitimate model owners. It is paramount to develop ownership protection methods to safeguard the intellectual property of a GAN model.

Despite confronting these threats, research on ownership protection for GANs is somehow much less explored. There is one work [26] that proposes a watermark-based method for protecting ownership of GANs, but it needs to utilize extra loss functions to retrain the model. More importantly, it only considers physical stealing, and emerging model extraction attacks are taken into consideration.

In this paper, we develop a new ownership protection method for GANs, which can protect ownership on both physical stealing and model extraction attacks. Our method claims the ownership of a GAN by leveraging common characteristics of a target model and its stolen models. The rationale for our method is that stolen models are derived from the target model while honest models are not. Thus, these common characteristics can be leveraged to differentiate stolen models from honest models. More specifically, we utilize generated samples from GANs to build a discriminative classifier to learn these characteristics. This is because the objective of a GAN is to learn the distribution of a training dataset and the learned implicit distribution of a GAN can be represented by these generated samples [2] (see Section 4.3).

We comprehensively evaluate our new method by comparing it with two state-of-the-art works: watermark-based method (abbreviation as Ong method) [26] and fingerprint-based method (abbreviation as Yu method) [40]. Here, note that fingerprint-based methods are proposed for deepfake detection and attribution [24, 34, 39–41]. In this work, we are the first to introduce them to the ownership protection field, considering their common objective: fingerprints can

be used to infer whether a suspect sample is from the model. Extensive experiments show that our method achieves the best performance in all evaluations among these ownership protection methods. In contrast, the other two methods cannot work in many cases, especially for model extraction attacks (see Section 6). Furthermore, we analyze the protection performance by visualizing the characteristics learned by our method (see Section 7.1). We also show the stability of our method on the number of generations of model extraction attacks, which is a new emerging threat in the generative domain. In contrast, the protection performance of the Yu method presents a significant linear decrease and the Ong method completely fails in providing any protection (see Section 7.2). Our analysis with respect to the number of generated samples and different datasets further shows the effectiveness of our method. Finally, extensive evaluations under adaptive attacks also demonstrate that our method is still effective and robust even if adversaries obtain partial knowledge of our method (see Section 8).

In summary, we make the following contributions. (1) We propose a novel ownership protection method GAN-Guards from a new perspective: detecting ownership infringement by utilizing the common characteristics of a target model and stolen models. (2) We evaluate our method on various attacks, including emerging model extraction attacks. (3) Our method achieves a new state-of-the-art performance in ownership protection for GANs compared to prior works. The source code will be made public along with the final version of the paper.

## 2. Related Work

**Generative adversarial networks.** Generative adversarial networks (GANs) have undoubtedly achieved a series of successes in image generation [3, 16–18, 25], image manipulation [30, 31], and image super-resolution [19, 43]. The seminal GAN introduced in 2014 [10] presents a promising result in image synthesis, which significantly inspires more and more researchers to propose various methods to further advance the performance of GANs. Karras et al. [16] propose a progressive training strategy that enables a GAN to synthesize high-resolution images. In addition to generating high-resolution images, Karras et al. [17] further introduce neural style transfer structures into the architecture of GANs and it empowers GANs to generate a variety of style images. Takeru et al. [25] introduce spectral normalization to normalize the weights of each layer to improve the quality of synthetic images. *Overall, each improvement in GANs requires talented researchers to devote tremendous efforts. In this work, instead of further improving the performance of GANs, we target at developing a technique to protect the intellectual property of valuable GANs.*

**Ownership protection.** There are numerous works aiming to protect ownership of discriminative models [4, 6, 7, 15,

20, 21, 33, 42]. These works can be generally classified into three groups: embedding watermarks into model parameters [33], using predefined inputs as triggers [1] and utilizing unique features of models [4, 23]. *However, methods on discriminative models cannot be applied to generative models since they are different machine learning models.*

There are only a few works on ownership protection of generative models. Ong et al. [26] propose a protection framework for GANs by adding a novel regularization term to the existing loss function. Some works on fingerprints of GANs can be applied into this field. Yu et al. [40] propose to add fingerprints into training data and then verify the fingerprints on GANs. Additionally, Yu et al. [41] add a novel fingerprint embedding layer to modulate the generation of fingerprinted images. *However, these works do not perform evaluations on emerging model extraction attacks. In this work, we propose a novel protection method and thoroughly evaluate these works on various attacks, including model extraction attacks.*

## 3. Background

### 3.1. Generative Adversarial Networks

An unconditional GAN generally consists of a generator  $G$  and a discriminator  $D$ . In the training phase, the generator  $G$  aims to generate fake data to fool the discriminator  $D$  while the discriminator  $D$  attempts to distinguish fake data from the generator from the real data from the training set. Once finishing training, the generator  $G$  can be utilized to generate data, given latent codes. Gaussian distribution or uniform distribution is commonly used to obtain latent codes. Mathematically, the generator of a GAN is a function  $G : \mathcal{Z} \rightarrow \mathcal{X}$  that maps a low dimensional latent space  $\mathcal{Z} \subseteq \mathbb{R}^n$  to a high dimension data space  $\mathcal{X} \subseteq \mathbb{R}^m$ .

### 3.2. Paradigms of Ownership Protection

Current paradigms of ownership protection on GANs can be divided into two classes: watermark-based methods and fingerprint-based methods. Watermark-based methods initially are proposed in the work [26]. The key idea is that model owners claim ownership of this GAN if special outputs can be obtained from a suspect GAN. Generally, these special outputs (e.g. watermarked generated samples) are obtained through special queries from a GAN. For simplicity, we refer to this ownership protection method by the first author’s name, i.e. Ong [26].

Fingerprint-based methods are initially proposed for deepfake detection and attribution [40, 41]. In this work, we apply these methods to protect ownership of GANs. This is because they share a common objective that fingerprints can be used to infer whether a suspect sample is from their model. Specifically, the key idea of fingerprint-based methods is that if the fingerprint extracted from generated sam-

ples from a GAN is identical to the true fingerprint, model owners can claim ownership of the GAN. To achieve this goal, various methods are proposed, such as adding fingerprints on the training set of a GAN [40], and designing new architectures of a GAN and loss functions [41]. In this work, considering the flexibility and scalability of a method, we choose the former method—Yu [40] to evaluate the performance in ownership protection and make a comparison with our proposed method.

Note that, unlike these paradigms that require forcibly implanting watermarks/fingerprints into target models and retraining target models, our method provides a novel paradigm: the common characteristics of a target model and its stolen models are exploited to claim ownership, motivated by the emerging of model extraction attacks.

## 4. A New Ownership Protection Method

### 4.1. Threat Model

We assume that defenders, i.e. model providers who deploy an ownership protection method on their target model, only have access to generated samples from a suspect model deployed by the adversaries. Thus, the defenders make an ownership infringement decision only based on these generated samples. *This is the most practical and strictest assumption for defenders.*

### 4.2. Key Observations

The first key observation is that physical stealing and model extraction attacks are two fundamental but different types of ownership infringement. Physical stealing attacks refer that an adversary physically copies a model  $G_{sub}$  from the target model  $G_{tar}$ . Therefore,  $G_{sub}$  is totally the same as  $G_{tar}$ . Model extraction attacks [13] refer that an adversary retrains a substitute model  $G_{sub}$  on generated samples from a target model  $G_{tar}$ . These generated samples can be obtained by an adversary when model owners release generated samples or provide a querying interface. Thus,  $G_{sub}$  is functionally similar to  $G_{tar}$ .

The second key observation is that as stolen models (i.e. constructed by physical stealing or model extraction attacks) are derived from the target model but honest models are not, it is thus natural to assume that stolen models and the target model share common characteristics which do not exist in honest models. Therefore, we can learn and leverage such characteristics as an evidence to differentiate stolen models from honest models.

### 4.3. Ownership Protection Algorithm

**Overview.** In order to extract the characteristics for a target model, our method proposes to learn these characteristics by training a binary classifier on generated samples. Generated samples from model extraction and physical stealing

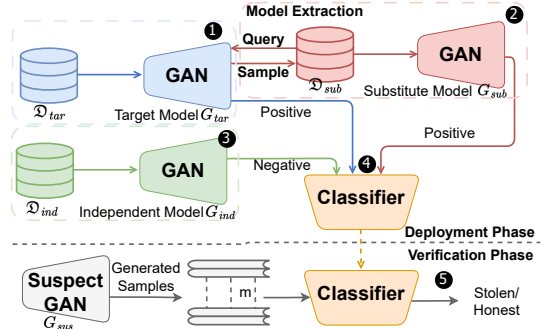


Figure 1: Overview of our method. **1** A target model is trained on a dataset  $\mathcal{D}_{tar}$ . **2** A substitute model is constructed by model extraction. **3** An independent model is trained on a dataset  $\mathcal{D}_{ind}$  that has the same distribution as the dataset  $\mathcal{D}_{tar}$ , but it is disjoint with  $\mathcal{D}_{tar}$ . **4** A classifier is trained to discriminate between stolen models and honest models. **5** The classifier is used for the verification of a suspect model. Here, the target model can also refer to the physically stealing model. The defenders do not have any information about a suspect model  $G_{sus}$ , except generated samples, in the verification phase.

are labelled as positive while samples from honest models, i.e. independently trained models, are labelled as negative. The reason why we use generated samples is that a GAN model is to learn the distribution of a training set. The learned distribution is implicit, which can be represented through these generated samples [2]. This process is shown in the deployment phase of Figure 1.

In practice, it is impossible for the defenders to consider all independently trained models and all models constructed by model extraction. Therefore, our method constructs positive and negative GAN models only by the limited knowledge of the defenders: the architectures of the target model and the training set. Specifically, the architectures of all models (i.e.  $G_{tar}$ ,  $G_{sub}$ ,  $G_{ind}$ ) in the deployment phase are the same. The independent set  $\mathcal{D}_{ind}$  and the target set  $\mathcal{D}_{tar}$  are from the same distribution but disjoint.  $\mathcal{D}_{ind}$  can be easily obtained, e.g. the defenders split a dataset into two parts: one as the independent set and the other as the training set. We emphasize that our method is practical as suspect models constructed by the adversaries can be trained on any (unknown for the defenders) GAN architectures and datasets. Our extensive experiments in Section 6.4, demonstrate our method can well generalize beyond these unknown GANs and correctly recognize them.

**Algorithm.** As illustrated in the function *buildProtection* of Algorithm 1, specifically, given the generator of a target model  $G_{tar}$  and an independent dataset  $\mathcal{D}_{ind}$ , we first construct a substitute model  $G_{sub}$  by extracting the target model  $G_{tar}$ . Next, we train a GAN  $G_{ind}$  on the independent dataset  $\mathcal{D}_{ind}$ . Samples from  $G_{sub}$  and  $G_{tar}$  are labeled

---

**Algorithm 1: The GAN-Guards Algorithm.**

---

**Input:** a target model:  $G_{tar}$ ; an independent dataset  $\mathcal{D}_{ind}$ ;  
 $m$  samples  $X_{sus}$  from a suspect model  $G_{sus}$ .  
**Output:** ownership decision:  $OwDecision$

```
1 def buildProtection( $G_{tar}, \mathcal{D}_{ind}$ ):
2   Sample  $\tilde{n}$  samples  $X_{gen}$  from  $G_{tar}$ ;
3    $G_{sub} \leftarrow \text{trainGAN}(X_{gen})$ ;
4    $G_{ind} \leftarrow \text{trainGAN}(\mathcal{D}_{ind})$ ;
5   Sample  $n$  samples  $X_{gen}$  from  $G_{tar}$ ; ▷ labelling
   positive for physical stealing.
6   Sample  $n$  samples  $X_{sub}$  from  $G_{sub}$ ; ▷ labelling
   positive for model extraction.
7   Sample  $2n$  samples  $X_{ind}$  from  $G_{ind}$ ; ▷ labelling
   negative for the honest model.
8    $Classifier \leftarrow \text{trainClassifier}(X_{gen}, X_{sub}, X_{ind})$ ;
9   return  $Classifier$ 

10 def performVerification( $Classifier, X_{sus}, \tau$ ):
11   Initialize prediction array  $pred$  of length  $m$  with 0;
12   for  $i = 0$  to  $m - 1$  do
13      $pred[i] \leftarrow Classifier(X_{sus}[i])$ ; ▷ Prediction: 1
     or 0.
14    $ConfiScore = \text{sum}(pred)/m$ ;
15   ▷ Make a decision based on multiple samples.
16   if  $ConfiScore > \tau$  then  $OwDecision = 1$ ;
17   else  $OwDecision = 0$ ;
18   return  $OwDecision$ 
```

---

as positive while samples from  $G_{ind}$  are labeled as negative. These samples are used for training a classifier and in this work we choose ResNet50 [11] as the classifier.

After obtaining the trained classifier, we start to perform the verification of ownership. We first collect  $m$  generated samples released by a suspect model  $G_{sus}$ . These samples are fed into the classifier and  $m$  predictions can be obtained. We calculate the percentage of these positive predictions. If it is larger than a predefined threshold, the suspect model is inferred as stealing from the target model. We also analyze how the number of generated samples  $m$  affects our performance in Section 7.3. This process is also illustrated in the function *performVerification* of Algorithm 1.

## 5. Experiments

### 5.1. Datasets

We evaluate our method on two datasets: FFHQ [17] and Church [38]. They are typically used in image generation. The FFHQ dataset is designed for human face image synthesis and includes 70,000 images. The Church dataset is from the LSUN dataset, which contains 126,277 outdoor church images.

All images are resized to  $64 \times 64$ . For each dataset, we randomly split the dataset into three disjoint equal parts and mark each part as the corresponding dataset name plus ‘I’, ‘II’, and ‘III’, respectively, such as FFHQ-I and FFHQ-II.

Dataset I, i.e.  $\mathcal{D}_{tar}$ , is used to train a target GAN model. Dataset II is used to train a GAN and later the model (i.e. Ind-a in Section 5.2) is used as negative to test the ownership protection methods. Dataset III, i.e.  $\mathcal{D}_{ind}$ , is used to train a GAN model and later the model is used for building a classifier together with the target model. Specifically, we set the size of each part of FFHQ and Church as 20,000 and 40,000, respectively.

### 5.2. Suspect Models

We consider various suspect models. Positive suspect models are considered ownership infringement and these models are derived from the target models via physical stealing and model extraction, and obfuscation attacks, such as input perturbation, output perturbation, overwriting, and fine-tuning attacks. Negative suspect models are host models and they are built from independent training. Here, we consider two types: *Ind-a* trained on dataset II with the same architectures of target models, and *Ind-b* that is trained on dataset I, with the same architectures of target models but uses different seeds, i.e. different random initializations. In Section A.6 in Appendix, we detail the implementation and report performance of these suspect models.

### 5.3. Metrics

We use FID [12] to measure the performance of a GAN. 50K generated samples from a GAN and all training samples are used to compute the FID value.

In terms of protection performance, the Ong method [26] utilizes the SSIM [35] score to measure the similarity between the groundtruth watermark and the watermark extracted from a suspect model. If the SSIM score of an image is higher than a threshold, the image is more likely from the target model. The Yu method [40] calculates a bitwise accuracy between the groundtruth fingerprint and an extracted fingerprint. Claiming ownership of a model based on only one image is not robust enough. Therefore, we make a final decision by computing a confidence score on multiple samples. Specifically, given  $m$  samples and each sample gets an output  $o \in \{0, 1\}$  from a suspect method, the confidence score that recognizes a suspect model as positive is computed by:  $ConfidenceScore = \frac{\sum_{i=0}^{m-1} o_i}{m}$ . In this work, we set threshold  $\tau$  of all methods as 90% for consistency. Thus, a suspect model is predicted as positive (stolen model) if  $\tau \geq 90\%$ . We fix the number of samples  $m$  as 1,000.

### 5.4. Experimental Setups

In terms of GANs, we use SNGAN [25], PGGAN [16] and StyleGAN [17]. These all can achieve excellent performance in image synthesis. We use the official implementation of each GAN to train GANs. For model extraction attacks, considering a trade-off between attack cost and



Table 1: Performance of target model SNGAN trained on FFHQ-I on different methods. ( $\downarrow$  is better).

| Methods                                      | Ong   | Yu    | Ours  |
|--|-------|-------|-------|
| FID( $\mathcal{Q}, \tilde{G}$ ) $\downarrow$ | 20.14 | 26.46 | 20.25 |

performance, we set the number of generated samples as 50,000, which is also suggested by the work [13].

For our protection method, we use ResNet50 [11] pre-trained on ImageNet [27] dataset for our classifier. The SGD optimizer with a learning rate of 0.003 is used and the number of epochs is fixed as 5. As shown in Algorithm 1, we use the Gaussian prior distribution to obtain generated samples and the number of samples  $n$  is set as 100,000. Therefore, 400,000 samples in total are used for training the classifier. For the Ong method [26] and the Yu method [40], we adopt their official implementations with suggested hyperparameters.

## 6. Evaluation

In this section, we compare our method with two state-of-the-art methods: the Ong method [26] and the Yu method [40], and both have been already discussed in Section 3.2. We evaluate them from various perspectives, including model utility, verification performance, robustness to obfuscations, and robustness to more model extractions.

### 6.1. Model Utility

Table 1 shows the performance of the target model SNGAN trained on FFHQ-I with different protection methods. The FID is computed by the original training set  $\mathcal{Q}$  and the protected GAN  $\tilde{G}$ . Overall, the watermark-based method Ong and our method achieve similar outstanding performance, while the fingerprint-based method Yu shows worse performance. This is because the Yu method needs to add fingerprints into a training set, which is at the cost of sacrificing model utility.

### 6.2. Verification Performance

Figure 2 presents verification performance on different ownership protection methods. The red dashed line is the threshold  $\tau$  of the confidence score. A model is predicted as a stolen (positive) model if  $\tau \geq 90\%$ . PS refers to models from physical stealing while ME refers to models from model extraction. Note that here ME, Ind-a, Ind-b models used in the verification phase are not the same models used in our deployment phase (detailed in Section 5.2). Overall, our method can correctly differentiate all positive and negative suspect models, achieving 100% accuracy. However, the Ong method and the Yu method are unable to defend against model extraction attacks. Additionally, the Ong and Yu methods mistakenly recognize the suspect model Ind-b trained with different initializations as a stolen model. This

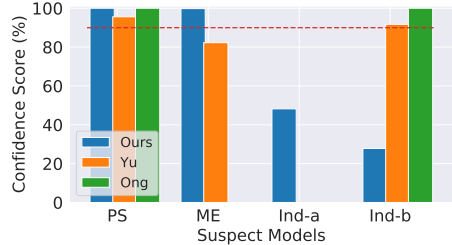


Figure 2: Verification performance of all methods. The target model SNGAN is trained on FFHQ-I. PS and ME are positive suspect models while Ind-a and Ind-b are negative suspect models. Note that *green and orange bars in some cases cannot be observed because their scores are 0%*.

is because embedded watermarks or fingerprints cannot be changed only owing to different initializations of a training process. Thus, their methods lead to false alarms and hurt honest model providers.

### 6.3. Robustness to Obfuscations

In order to evade verification, advanced adversaries may utilize obfuscation techniques to obfuscate stolen models. In this work, we consider four types of obfuscation techniques: input perturbation, output perturbation, overwriting and fine-tuning. Input perturbation aims to modify the queries, i.e., latent codes, to evade special queries. Here, we adopt random input perturbation. That is, for any query, a target model resamples latent codes from Gaussian distribution. For brevity, we rename it Inp. Output perturbation refers to perturbing generated samples by various post-processing techniques. We use four different output perturbations: additive Gaussian noise, Gaussian filter, Gaussian blurring, and JPEG compression. We briefly rename them Oup-a, Oup-b, Oup-c, and Oup-d, respectively. The magnitude of these perturbations is set as 0.01, 0.4, 0.5, and 0.85, respectively. Overwriting refers to encoding a different watermark/fingerprint to overwrite the original watermark/fingerprint. Our method does not rely on watermarks and fingerprints, thus intrinsically eliminating the threat of this attack. In this work, we consider wholly fine-tuning where we take the weights of the stolen model as initialization and retrain a GAN model on a different dataset FFHQ-II. Because these obfuscation operations can be added into physical stealing (PS) or model extraction (ME), there are different combinations between obfuscation operations and PS and ME. Here, we mark them as 'PS+' and 'ME+' corresponding obfuscation operations, such as PS+Inp. Implementations are illustrated in Section A.1 in Appendix.

**Results.** Figure 3 shows the protection performance under input and output perturbation operations. Overall, our method can still remain 100% accuracy against input perturbation and output perturbation attacks. In contrast, the Ong method totally cannot resist the input perturbation attack, as shown in Figure 3(a) and the Yu method cannot de-

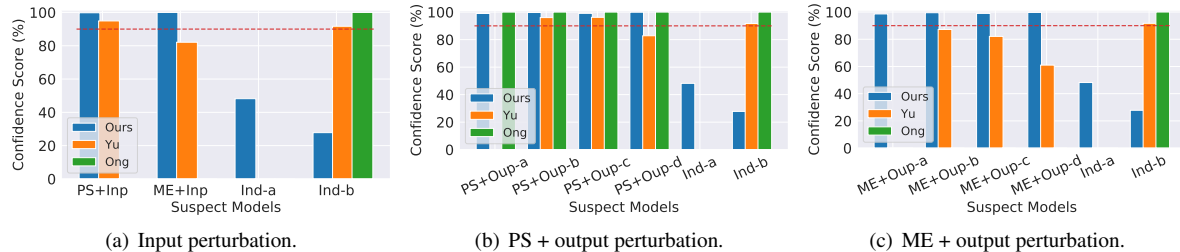


Figure 3: Robustness to Obfuscations. Protection performance for target model SNGAN trained on FFHQ-I. Again, green and orange bars in some cases cannot be observed because their scores are 0% and cannot defend against these attacks.

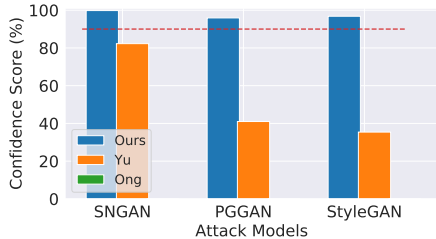


Figure 4: Protection performance under model extraction attacks with different GANs as attack models. The target model SNGAN is trained on FFHQ-I.

defend against additive Gaussian noise of output perturbation attacks (PS+Oup-a and ME+Oup-a). Again, Figure 3(c) shows that the Ong and Yu methods cannot defend against ME+Output perturbation. We analyze the reasons for the Ong and Yu methods in Section A.2 in Appendix.

We perform the evaluation under the overwriting attack. We do not report results for our method because our method does not rely on watermarks or fingerprints. Overall, the Ong and Yu methods cannot defend against this type of attack and both confidence scores are 0%. It indicates that the overwritten watermarks and fingerprints make their methods unable to extract the expected outputs. We summarize the results in Table 3 in Appendix.

We evaluate the protection performance under the fine-tuning attack. Unfortunately, we observe that all methods are not robust to the fine-tuning attack. We analyze that this is because the fine-tuned GAN model has learned a different distribution in a new training set and neural networks suffer from catastrophic forgetting [8, 9]. The former makes that our method recognizes this model as an independent training model while the latter makes that the Ong and Yu methods forget embedded watermarks and fingerprints. This also inspires us to think about the ownership boundary of a GAN and develop more powerful protection work in future. We summarize the results in Table 4 in Appendix.

#### 6.4. Robustness to More Model Extraction

When mounting model extraction attacks, adversaries can utilize various architectures of GANs to extract a target model. Figure 4 shows the results of all methods in terms of

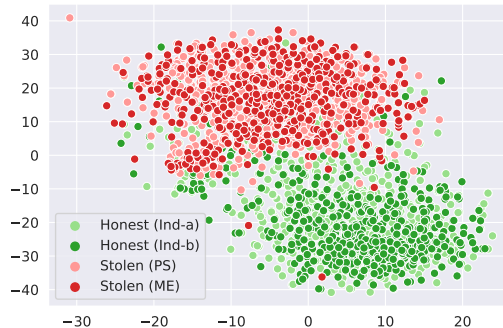


Figure 5: T-SNE visualization of characteristics learned by our method for stolen models and honest models.

robustness to model extraction attacks with different GANs as attack models. The target model is SNGAN. We see that our method still performs well, while the other two methods recognize them as honest models. *This shows our method can recognize models constructed by model extraction attacks regardless of the GAN architectures of adversaries.*

## 7. Analysis

### 7.1. Visualization of Characteristics

Figure 5 shows the T-SNE visualization of characteristics learned by our method. We plot the T-SNE figure by using outputs from the penultimate layer of the classifier and the dimension of the outputs is 2,048. We clearly see that characteristics from stolen models including PS and ME are entangled together and have a clear boundary with that from honest models.

### 7.2. Generations of Model Extraction Attacks

Theoretically, model extraction attacks on GANs can continue forever like the process of biological heredity, as shown in Figure 6. Models produced during this process, such as  $G^{(i)}$ , should be correctly identified by ownership protection methods. This motivates us to investigate whether the protection performance will decrease with the number of generations of model extraction attacks. We emphasize this is our newly identified threat, which is not discussed in the literature about GAN ownership protection.

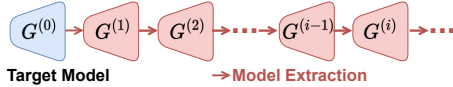


Figure 6: Generations of model extraction attacks.

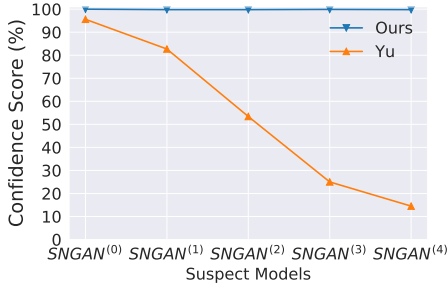


Figure 7: Protection performance with regard to the number of generations of model extraction attacks.

Here, we fix the number of generated samples as 1,000 and the target model is SNGAN trained on FFHQ-I. We mark the target model SNGAN as SNGAN<sup>(0)</sup>, and the first generation of model extraction is marked as SNGAN<sup>(1)</sup>, which means an adversary uses an attack model SNGAN to extract the target model SNGAN. We do not show the performance of the Ong method because it cannot defend against model extraction attacks.

As shown in Figure 7, we can clearly observe that with the increase in the number of generations of model extraction, the Yu method becomes less and less confident. It also indicates that the fingerprint is not robust and more and more generated samples cannot extract the corresponding fingerprint. In contrast, our method still remains almost 100% confident to verify ownership of the target model.

### 7.3. Number of Generated Samples

Figure 8 presents the protection performance of our method under the different numbers of generated samples. The target model SNGAN is trained on FFHQ-I. The ground truth of PS and ME is positive while that of Ind-a and Ind-b is negative. We can clearly see that the confidence scores gradually remain stable after 1,000 generated samples on all suspect models. It also shows that our protection method has advantages with respect to the *efficiency*, i.e. it requires as few as 1,000 samples.

### 7.4. Different Datasets

We now present the performance of our method on the Church dataset which is widely used in scene synthesis. The detail of this dataset is also discussed in Section 5.1. The target model is SNGAN trained on the Church-I dataset and achieves 12.96 FID.

Overall, our method on the Church dataset can achieve the same exceptional protection performance as that on the FFHQ dataset. Figure 9(a) shows verification performance

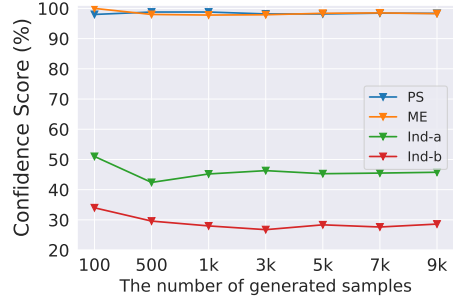


Figure 8: Protection performance with regard to the numbers of generated samples.

on our method. We can clearly observe that our method can verify the positive suspect models as positive with high confidence. As shown in Figure 9(b), Figure 9(c) and Figure 9(d), our method can still remain 100% accuracy under the input perturbation and output perturbation. Our method on fine-tuning attacks shows it fails to recognize positive suspect models as positive. We show details in Table 5 in Appendix, and we also analyze the performance on different target models in Section A.4.2 in Appendix.

## 8. Adaptive Attacks

Although researchers studying defense techniques strongly advocates that a new defense should be evaluated on adaptive attacks [32], prior works on ownership protection on GANs do not adopt it. In this work, for the first time, we present the performance of our method under adaptive attacks. That is, we assume that adversaries have some knowledge of our protection method, and design a series of specific attacks to evade our method.

We discuss two types of adaptive attack scenarios. The main design principle is that we assume that adversaries perceive our method which is based on the common characteristics of a target model and its stolen models. Therefore, the adversaries attempt to decrease the confidence score of our method by sacrificing model utility (i.e. the quality of generated images). Specifically, in adaptive attack I, adversaries choose an inferior performance GAN from multiple snapshots of a GAN when mounting model extraction attacks. In adaptive attack II, adversaries evade our verification by designing a series of output perturbations by choosing the magnitude of the perturbation.

Figure 10 shows protection performance under the adaptive attack I. Here, we choose an attack model SNGAN to extract the target model SNGAN trained on FFHQ-I. We choose eight snapshots of SNGAN during model extraction attacks. The performance of the attack model SNGAN, i.e.  $FID(p_g, p_{\bar{g}})$ , ranges from 22 to 2, as depicted in the red line.  $p_g$  and  $p_{\bar{g}}$  are the implicit distribution of the target model and the attack model, respectively. We can observe that confidence scores begin to decrease, then increase and remain at 100%, with the decrease in FID of the attack model

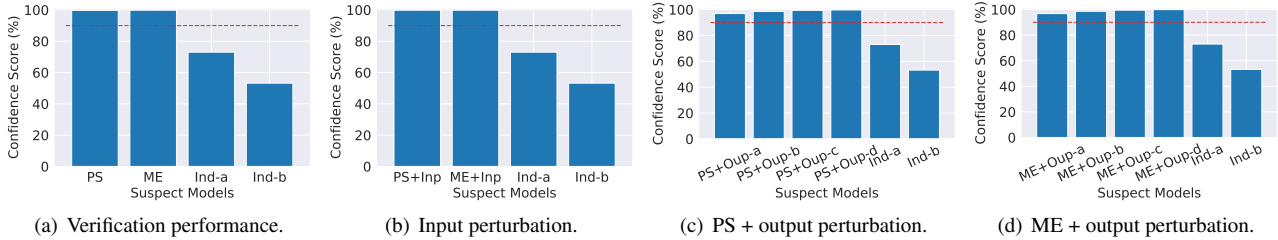


Figure 9: Protection performance on target model SNGAN trained on Church-I.

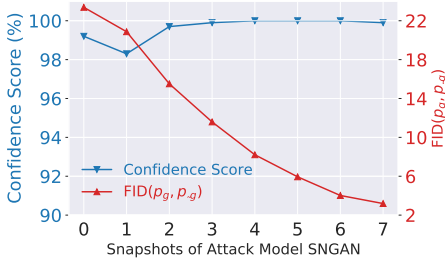


Figure 10: Protection performance under the adaptive attack I. The target model SNGAN is trained on FFHQ-I.

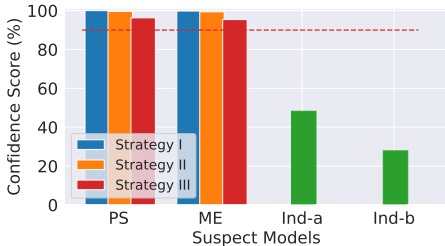


Figure 11: Protection performance under the adaptive attack II. The target model SNGAN is trained on FFHQ-I.

SNGAN. In particular, the confidence scores of all snapshots are above 98%, which indicates that our method can correctly recognize all snapshots as stolen models.

Figure 11 shows protection performance under the adaptive attack II. Considering the model utility, we design three strategies (strategy I, strategy II and strategy III) based on different magnitudes of four types of output perturbation. Table 2 summarizes the magnitudes of output perturbation of each strategy. Note that we combine four types of output perturbation instead of single output perturbation. In Figure 17 in Appendix, we visually present images generated by each strategy and the quality of generated images becomes much noisier and blurrier from strategy I to strategy III. Overall, we can observe in Figure 11 that our method still can recognize all positive suspect models, although the confidence score of each suspect model decreases from strategy I to strategy III. In addition, although strategy III can lower the confidence of our method, the model almost cannot be used due to the low quality of generated images visually. In practice, the loss in model utility

Table 2: Magnitudes of output perturbation of the adaptive attack II. a: Additive Gaussian Noise; b: Gaussian Filtering; c: Gaussian Blurring; d: JPEG Compression.

| Strategy | Output Perturbation |     |     |    |
|----------|---------------------|-----|-----|----|
|          | a                   | b   | c   | d  |
| I        | 0.001               | 0.1 | 0.1 | 95 |
| II       | 0.005               | 0.2 | 0.3 | 90 |
| III      | 0.01                | 0.4 | 0.5 | 85 |

can make the adversaries less competitive in market share, compared to legitimate model owners.

## 9. Conclusion

In this paper, we have proposed a novel method to protect GAN ownership by leveraging the common characteristics of a target model and its stolen GANs. Extensive experimental evaluations demonstrate that: (a) In terms of model utility, our method can bring lossless fidelity, compared to models without protection, because it does not modify well-trained target models. (b) In terms of robustness, our method can achieve new state-of-the-art protection performance, compared with watermark-based methods and fingerprint-based methods. Furthermore, we have also shown that our method is still effective under two types of carefully designed adaptive attacks. (c) In terms of undetectability, our method is undetectable for adversaries because it builds on a target model with normal training and does not rely on watermarks or fingerprints. (d) In terms of efficiency, our method requires about 1,000 generated samples to confidently verify the ownership of a GAN. Finally, we also have performed a fine-grained analysis of our method from various aspects, such as visualizing learned characteristics, the stability of the performance with regard to the number of generations of model extraction attacks, the number of generated samples and different datasets.

Fine-tuning attacks remain a challenge for ownership protection on GANs. In future, we plan to design more powerful methods to defend against these types of attacks. In addition, applying our protection method to other domains, such as table data synthesis and text generation, is also an interesting research direction.



## Acknowledgments

This research was funded in whole by the Luxembourg National Research Fund (FNR), grant reference 13550291.

## References

- [1] Yossi Adi, Carsten Baum, Moustapha Cisse, Benny Pinkas, and Joseph Keshet. Turning your weakness into a strength: Watermarking deep neural networks by backdooring. In *Proceedings of USENIX Security Symposium (USENIX Security)*, pages 1615–1631. USENIX Association, 2018. [2](#)
- [2] Yasaman Bahri, Jonathan Kadmon, Jeffrey Pennington, Sam S. Schoenholz, Jascha Sohl-Dickstein, and Surya Ganguli. Statistical mechanics of deep learning. *Annual Review of Condensed Matter Physics*, 11(1):501–528, 2020. [1](#), [3](#)
- [3] Andrew Brock, Jeff Donahue, and Karen Simonyan. Large scale GAN training for high fidelity natural image synthesis. In *Proceedings of International Conference on Learning Representations (ICLR)*, 2019. [1](#), [2](#)
- [4] Jialuo Chen, Jingyi Wang, Tinglan Peng, Youcheng Sun, Peng Cheng, Shouling Ji, Xingjun Ma, Bo Li, and Dawn Song. Copy, right? a testing framework for copyright protection of deep learning models. In *Proceedings of IEEE Symposium on Security and Privacy (S&P)*, pages 1013–1030. IEEE, 2022. [2](#)
- [5] Anton Cherepkov, Andrey Voynov, and Artem Babenko. Navigating the gan parameter space for semantic image editing. In *Proceedings of IEEE/CVF Conference on Computer Vision and Pattern Recognition (CVPR)*, pages 3671–3680. IEEE, 2021. [1](#)
- [6] Tianshuo Cong, Xinlei He, and Yang Zhang. Sslguard: A watermarking scheme for self-supervised learning pre-trained encoders. In *Proceedings of ACM SIGSAC Conference on Computer and Communications Security (CCS)*, pages 579–593. ACM, 2022. [2](#)
- [7] Adam Dziedzic, Haonan Duan, Muhammad Ahmad Kaleem, Nikita Dhawan, Jonas Guan, Yannis Cattan, Franziska Boenisch, and Nicolas Papernot. Dataset inference for self-supervised models. In *Proceedings of Annual Conference on Neural Information Processing Systems (NeurIPS)*. Curran Associates, Inc., 2022. [2](#)
- [8] Robert M French. Catastrophic forgetting in connectionist networks. *Trends in Cognitive Sciences*, 3(4):128–135, 1999. [6](#)
- [9] Ian Goodfellow, Mehdi Mirza, Da Xiao, Aaron Courville, and Yoshua Bengio. An empirical investigation of catastrophic forgetting in gradient-based neural networks. *arXiv preprint arXiv:1312.6211*, 2013. [6](#)
- [10] Ian Goodfellow, Jean Pouget-Abadie, Mehdi Mirza, Bing Xu, David Warde-Farley, Sherjil Ozair, Aaron Courville, and Yoshua Bengio. Generative adversarial nets. In *Proceedings of Annual Conference on Neural Information Processing Systems (NeurIPS)*, pages 2672–2680. Curran Associates, Inc., 2014. [1](#), [2](#)
- [11] Kaiming He, Xiangyu Zhang, Shaoqing Ren, and Jian Sun. Deep residual learning for image recognition. In *Proceedings of IEEE/CVF Conference on Computer Vision and Pattern Recognition (CVPR)*, pages 770–778. IEEE, 2016. [4](#), [5](#)
- [12] Martin Heusel, Hubert Ramsauer, Thomas Unterthiner, Bernhard Nessler, and Sepp Hochreiter. Gans trained by a two time-scale update rule converge to a local nash equilibrium. In *Proceedings of Annual Conference on Neural Information Processing Systems (NeurIPS)*, pages 6626–6637. Curran Associates, Inc., 2017. [4](#)
- [13] Hailong Hu and Jun Pang. Stealing machine learning models: Attacks and countermeasures for generative adversarial networks. In *Annual Computer Security Applications Conference (ACSAC)*, pages 1–16. ACM, 2021. [1](#), [3](#), [5](#), [13](#), [14](#)
- [14] Phillip Isola, Jun-Yan Zhu, Tinghui Zhou, and Alexei A Efros. Image-to-image translation with conditional adversarial networks. In *Proceedings of IEEE/CVF Conference on Computer Vision and Pattern Recognition (CVPR)*, pages 1125–1134. IEEE, 2017. [1](#)
- [15] Hengrui Jia, Christopher A Choquette-Choo, Varun Chandrasekaran, and Nicolas Papernot. Entangled watermarks as a defense against model extraction. In *Proceedings of USENIX Security Symposium (USENIX Security)*, pages 1937–1954. USENIX Association, 2021. [2](#)
- [16] Tero Karras, Timo Aila, Samuli Laine, and Jaakko Lehtinen. Progressive growing of GANs for quality, stability, and variation. In *Proceedings of International Conference on Learning Representations (ICLR)*, 2018. [2](#), [4](#)
- [17] Tero Karras, Samuli Laine, and Timo Aila. A style-based generator architecture for generative adversarial networks. In *Proceedings of IEEE/CVF Conference on Computer Vision and Pattern Recognition (CVPR)*, pages 4401–4410. IEEE, 2019. [1](#), [2](#), [4](#)
- [18] Tero Karras, Samuli Laine, Miika Aittala, Janne Hellsten, Jaakko Lehtinen, and Timo Aila. Analyzing and improving the image quality of stylegan. In *Proceedings of IEEE/CVF Conference on Computer Vision and Pattern Recognition (CVPR)*, pages 8110–8119. IEEE, 2020. [2](#)
- [19] Christian Ledig, Lucas Theis, Ferenc Huszár, Jose Caballero, Andrew Cunningham, Alejandro Acosta, Andrew Aitken, Alykhan Tejani, Johannes Totz, Zehan Wang, et al. Photo-realistic single image super-resolution using a generative adversarial network. In *Proceedings of IEEE/CVF Conference on Computer Vision and Pattern Recognition (CVPR)*, pages 4681–4690, 2017. [2](#)
- [20] Zheng Li, Chengyu Hu, Yang Zhang, and Shanqing Guo. How to prove your model belongs to you: A blind-watermark based framework to protect intellectual property of dnn. In *Annual Computer Security Applications Conference (ACSAC)*, pages 126–137. ACM, 2019. [2](#)
- [21] Nils Lukas, Yuxuan Zhang, and Florian Kerschbaum. Deep neural network fingerprinting by conferrable adversarial examples. In *Proceedings of International Conference on Learning Representations (ICLR)*, 2021. [2](#)
- [22] Shuang Ma, Jianlong Fu, Chang Wen Chen, and Tao Mei. Da-gan: Instance-level image translation by deep attention generative adversarial networks. In *Proceedings of IEEE/CVF Conference on Computer Vision and Pattern Recognition (CVPR)*, pages 5657–5666. IEEE, 2018. [1](#)

- [23] Pratyush Maini, Mohammad Yaghini, and Nicolas Papernot. Dataset inference: Ownership resolution in machine learning. In *Proceedings of International Conference on Learning Representations (ICLR)*, 2020. [2](#)
- [24] Francesco Marra, Diego Gragnaniello, Luisa Verdoliva, and Giovanni Poggi. Do gans leave artificial fingerprints? In *2019 IEEE conference on multimedia information processing and retrieval (MIPR)*, pages 506–511. IEEE, 2019. [1](#)
- [25] Takeru Miyato, Toshiki Kataoka, Masanori Koyama, and Yuichi Yoshida. Spectral normalization for generative adversarial networks. In *Proceedings of International Conference on Learning Representations (ICLR)*, 2018. [1](#), [2](#), [4](#)
- [26] Ding Sheng Ong, Chee Seng Chan, Kam Woh Ng, Lixin Fan, and Qiang Yang. Protecting intellectual property of generative adversarial networks from ambiguity attacks. In *Proceedings of IEEE/CVF Conference on Computer Vision and Pattern Recognition (CVPR)*, pages 3630–3639. IEEE, 2021. [1](#), [2](#), [4](#), [5](#)
- [27] Olga Russakovsky, Jia Deng, Hao Su, Jonathan Krause, Sanjeev Satheesh, Sean Ma, Zhiheng Huang, Andrej Karpathy, Aditya Khosla, Michael Bernstein, Alexander C. Berg, and Li Fei-Fei. Imagenet large scale visual recognition challenge. *International Journal of Computer Vision*, 115(3):211–252, 2015. [5](#)
- [28] Axel Sauer, Katja Schwarz, and Andreas Geiger. Stylegan-xl: Scaling stylegan to large diverse datasets. In *Proceedings ACM SIGGRAPH Conference (SIGGRAPH '22)*, pages 1–10. ACM, 2022. [1](#)
- [29] E Eugene Schultz. A framework for understanding and predicting insider attacks. *Computers & Security*, 21(6):526–531, 2002. [1](#)
- [30] Yujun Shen, Jinjin Gu, Xiaou Tang, and Bolei Zhou. Interpreting the latent space of gans for semantic face editing. In *Proceedings of IEEE/CVF Conference on Computer Vision and Pattern Recognition (CVPR)*, pages 9243–9252. IEEE, 2020. [2](#)
- [31] Yujun Shen and Bolei Zhou. Closed-form factorization of latent semantics in gans. In *Proceedings of IEEE/CVF Conference on Computer Vision and Pattern Recognition (CVPR)*, pages 1532–1540. IEEE, 2021. [1](#), [2](#)
- [32] Florian Tramer, Nicholas Carlini, Wieland Brendel, and Aleksander Madry. On adaptive attacks to adversarial example defenses. In *Proceedings of Annual Conference on Neural Information Processing Systems (NeurIPS)*, volume 33, pages 1633–1645. Curran Associates, Inc., 2020. [7](#)
- [33] Yusuke Uchida, Yuki Nagai, Shigeyuki Sakazawa, and Shin’ichi Satoh. Embedding watermarks into deep neural networks. In *Proceedings of ACM International Conference on Multimedia Retrieval (ICMR)*, pages 269–277. ACM, 2017. [2](#)
- [34] Sheng-Yu Wang, Oliver Wang, Richard Zhang, Andrew Owens, and Alexei A Efros. Cnn-generated images are surprisingly easy to spot... for now. In *Proceedings of IEEE/CVF Conference on Computer Vision and Pattern Recognition (CVPR)*, pages 8695–8704. IEEE, 2020. [1](#)
- [35] Zhou Wang, Alan C Bovik, Hamid R Sheikh, and Eero P Simoncelli. Image quality assessment: from error visibility to structural similarity. *IEEE Transactions on Image Processing*, 13(4):600–612, 2004. [4](#)
- [36] Weihao Xia, Yulun Zhang, Yujiu Yang, Jing-Hao Xue, Bolei Zhou, and Ming-Hsuan Yang. Gan inversion: A survey. *IEEE Transactions on Pattern Analysis and Machine Intelligence*, 2022. [1](#)
- [37] Zili Yi, Hao Zhang, Ping Tan, and Minglun Gong. Dualgan: Unsupervised dual learning for image-to-image translation. In *Proceedings of IEEE International Conference on Computer Vision (ICCV)*, pages 2849–2857. IEEE, 2017. [1](#)
- [38] Fisher Yu, Ari Seff, Yinda Zhang, Shuran Song, Thomas Funkhouser, and Jianxiong Xiao. LSUN: Construction of a large-scale image dataset using deep learning with humans in the loop. *arXiv preprint arXiv:1506.03365*, 2015. [4](#)
- [39] Ning Yu, Larry S Davis, and Mario Fritz. Attributing fake images to gans: Learning and analyzing gan fingerprints. In *Proceedings of IEEE International Conference on Computer Vision (ICCV)*, pages 7556–7566. IEEE, 2019. [1](#)
- [40] Ning Yu, Vladislav Skripniuk, Sahar Abdelnabi, and Mario Fritz. Artificial fingerprinting for generative models: Rooting deepfake attribution in training data. In *Proceedings of IEEE International Conference on Computer Vision (ICCV)*, pages 14448–14457. IEEE, 2021. [1](#), [2](#), [3](#), [4](#), [5](#)
- [41] Ning Yu, Vladislav Skripniuk, Dingfan Chen, Larry S. Davis, and Mario Fritz. Responsible disclosure of generative models using scalable fingerprinting. In *Proceedings of International Conference on Learning Representations (ICLR)*, 2022. [1](#), [2](#), [3](#)
- [42] Jialong Zhang, Zhongshu Gu, Jiyong Jang, Hui Wu, Marc Ph Stoecklin, Heqing Huang, and Ian Molloy. Protecting intellectual property of deep neural networks with watermarking. In *Proceedings of the Asia Conference on Computer and Communications Security (ASIACCS)*, pages 159–172. ACM, 2018. [2](#)
- [43] Wenlong Zhang, Yihao Liu, Chao Dong, and Yu Qiao. Ranksgan: Generative adversarial networks with ranker for image super-resolution. In *Proceedings of IEEE/CVF Conference on Computer Vision and Pattern Recognition (CVPR)*, pages 3096–3105. IEEE, 2019. [2](#)
- [44] Jiapeng Zhu, Yujun Shen, Deli Zhao, and Bolei Zhou. In-domain gan inversion for real image editing. In *Proceedings of European conference on computer vision (ECCV)*, pages 592–608. Springer, 2020. [1](#)
- [45] Jun-Yan Zhu, Taesung Park, Phillip Isola, and Alexei A Efros. Unpaired image-to-image translation using cycle-consistent adversarial networks. In *Proceedings of IEEE International Conference on Computer Vision (ICCV)*, pages 2223–2232. IEEE, 2017. [1](#)

## A. Appendix

### A.1. Details of Obfuscations

In this subsection, we introduce obfuscation operations, including input perturbation, output perturbation, overwriting, and fine-tuning.

*Input perturbation.* Given a trained GAN model  $G$ , we can get a generated sample  $x_g$  from the GAN by a latent code  $z$  which is drawn from prior distribution  $P$ , i.e.,  $x_g = G(z), z \sim P$ . Input perturbation aims to modify the queries, i.e., latent codes. The reason why we consider this is that some works verify the ownership by specific latent codes  $z' = T(z)$ .  $T$  is a function to transform a normal latent code  $z$  to a specific latent code  $z'$ . Therefore, an adversary can perturb latent codes to evade this type of verification. In this work, we adopt random input perturbation. Specifically, for any query, a target model resamples latent codes from Gaussian distribution.

*Output perturbation.* In addition to perturbing latent codes, an adversary can perturb generated samples. In this work, we consider the following four common operations.

- Random Noise.* This operation adds noises into a generated sample  $x_g$ . Common noises include Gaussian noise and Poisson noise. In this work, we choose Gaussian noise and the mean  $\mu$  and the variance  $\sigma$  control the strength of noises.
- Filtering.* This operation aims to enhance some characteristics of an image. Common operations include mean filter, median filter and Gaussian filter. In this work, we choose the Gaussian filter.
- Blurring.* This operation makes a generated sample  $x_g$  less sharp by convolution. Common blurring operations include box blurring and Gaussian blurring. In this work, we choose Gaussian blurring.
- Compression.* This operation is to compress the size of an image without significantly degrading the image quality. Common compression operations include lossless compression JPEG and lossy compression JPG. In this work, we choose JPEG compression.

*Overwriting.* This attack is to target a class of ownership protection methods utilizing watermarks or fingerprints. An adversary can encode a different watermark/fingerprint to overwrite the original watermark/fingerprint. Ideally, an ownership protection method should still verify the ownership in this case. In this work, our proposed method does not rely on watermarks and fingerprints, thus intrinsically eliminating the threat of this attack.

*Fine-tuning.* After obtaining a substitute model, an adversary may further fine-tune the model on their own dataset.



Figure 12: Watermarks under different output perturbations. (a) is the original watermark. From (b) to (e), the output perturbation operations are Additive Gaussian Noise, Gaussian Filtering, Gaussian Blurring, and JPEG Compression, respectively. The corresponding SSIM scores between (a) and each output perturbation are 84.085%, 97.47%, 99.34%, 95.43%, respectively.

### DNN

Figure 13: Watermarks used for overwriting attacks.

Generally, an adversary can partially or wholly fine-tune the model. Wholly fine-tuning refers that all weights of the model are fine-tuned while partially fine-tuning refers that the weights of some layers are frozen and the remaining are fine-tuned. In this work, we consider wholly fine-tuning in which we take the weights of the stolen model as initialization and retrain a GAN model on a new dataset FFHQ-II.

### A.2. Understanding In-depth

Figure 12 shows SSIM scores of watermarks under different output perturbations. Specifically, Figure 12 (a) is the watermark used in the Ong method. Figure 12 (b) - Figure 12 (e) show the watermark under different output perturbations. We can observe that only if the Ong method can extract watermarks, output perturbation attacks do not have a significant impact on the final decision. This can explain the reason why the Ong Method on PS+output perturbation can perform well, as shown in Figure 3(b).

However, model extraction attacks and their derivative attacks (i.e. ME+obfuscations) make the Ong and Yu methods fail. This is because these attacks severely undermine watermarks and fingerprints. It also indicates that methods based on watermarks and fingerprints are not robust and too easily perturbed.

### A.3. Additional Results in Section 6

#### A.3.1 Performance on overwriting attacks

Figure 13 shows a new watermark that is used for overwriting attacks for the Ong method. The original watermark is shown in Figure 12 (a).

Table 3 presents protection performance under the overwriting attacks. We do not show results for our method because our method does not rely on watermarks or fin-

Table 3: Protection performance on overwriting. The target model SNGAN is trained on FFHQ-I. The suspect model PS is the model obtained by physical stealing. Confi.: confidence; Pred.: prediction.

| Types | Ong             |       | Yu              |       |
|-------|-----------------|-------|-----------------|-------|
|       | Confi. Score(%) | Pred. | Confi. Score(%) | Pred. |
| PS    | 0.00            | 0     | 0.00            | 0     |

Table 4: Protection performance on fine-tuning. Target model SNGAN is trained on FFHQ-I.

| Types | Ong             |       | Yu              |       | Ours            |       |
|-------|-----------------|-------|-----------------|-------|-----------------|-------|
|       | Confi. Score(%) | Pred. | Confi. Score(%) | Pred. | Confi. Score(%) | Pred. |
| PS    | 0.00            | 0     | 0.00            | 0     | 40.10           | 0     |
| ME    | 0.00            | 0     | 0.00            | 0     | 28.00           | 0     |

gerprints. Here, we only choose the PS model obtained by physical stealing because it can be perfectly recognized by both methods on physical stealing attacks. Intuitively, the protection method cannot verify this suspect PS model, which also means that other suspect models cannot be correctly verified. We observe that the Ong and Yu methods cannot defend against this type of attack.

### A.3.2 Performance on fine-tuning attacks

We adopt wholly fine-tuning where all weights of each model are fine-tuned on FFHQ-II. Specifically, we take the weights of the stolen model as initialization and retrain a GAN model on FFHQ-II.

Table 4 reports protection performance under the fine-tuning attack. We observe that all protection methods cannot be robust against this attack. The main reason is that fine-tuning enforces a GAN to learn the distribution of a new dataset. Due to the catastrophic forgetting of a neural network, previously embedded information, such as watermarks and fingerprints, cannot be kept. Similarly, the fine-tuned GAN that has learned a new distribution is no longer similar to the target model, which fails our method.

## A.4. Additional Results in Section 7

### A.4.1 Performance on different datasets

Table 5 shows the protection performance of our method on fine-tuning attacks. We take the weights of the stolen model as initialization and retrain a GAN model on Church-II. Our evaluation shows that it fails to recognize positive suspect models as positive.

Figure 14 shows the results of our method in terms of robustness to different model extractions. We observe that our method still performs perfectly regardless of the types of attack models.

Table 5: Protection performance on fine-tuning. Target model SNGAN is trained on Church-I.

| Types | Confi. Score(%) | Pred. |
|-------|-----------------|-------|
| PS    | 50.50           | 0     |
| ME    | 46.40           | 0     |

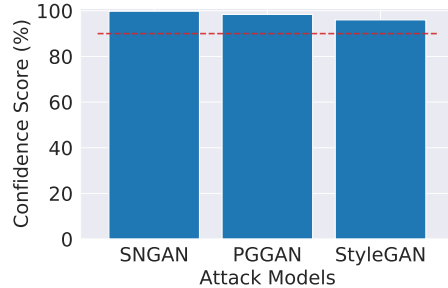


Figure 14: Robustness to more model extraction attacks. Protection performance under model extraction attacks with different GANs as attack models. Target model SNGAN is trained on Church-I.

Table 6: Protection performance on fine-tuning. Target model StyleGAN is trained on FFHQ-I.

| Types | Confi. Score(%) | Pred. |
|-------|-----------------|-------|
| PS    | 35.90           | 0     |
| ME    | 49.40           | 0     |

### A.4.2 Performance on different target models

We also show the protection performance of our method on the target model StyleGAN. The StyleGAN is trained on FFHQ-I and achieves 8.76 FID.

Overall, our method still has competitive protection performance on the target model StyleGAN. Our method can achieve 100% accuracy on verification performance for all suspect models, as shown in Figure 15(a). In terms of obfuscations, 100% accuracy can be seen on input perturbation attacks and four types of output perturbation attacks, as depicted in Figure 15(b), Figure 15(c) and Figure 15(d) respectively. In the face of fine-tuning attacks, we can see in Table 6 that our method still fails to recognize these positive suspect models. Figure 16 shows the results of our method in terms of robustness to different model extractions. We observe that our method still performs perfectly regardless of the types of attack models.

## A.5. Image Quality under Adaptive Attack II

Figure 17 shows the image quality of three strategies under adaptive attack II. Adversaries need to trade off model utility, i.e. the quality of generated images, and copyright infringement risks. Although a large magnitude output perturbation can help adversaries evade ownership detection, it will lower model utility. It also makes the stolen models less competitive, compared to the target models.



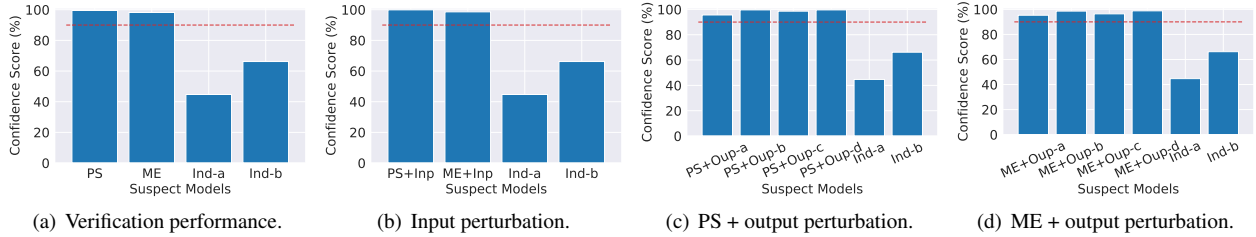


Figure 15: Protection performance on target model StyleGAN trained on FFHQ-I.

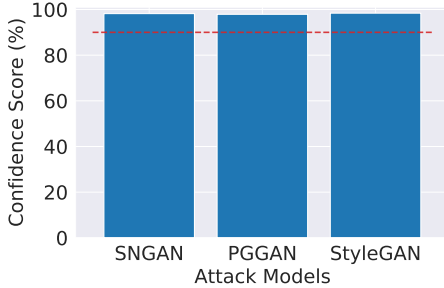


Figure 16: Robustness to more model extraction. Protection performance under model extraction with different GANs as attack models. Target model StyleGAN is trained on FFHQ-I.

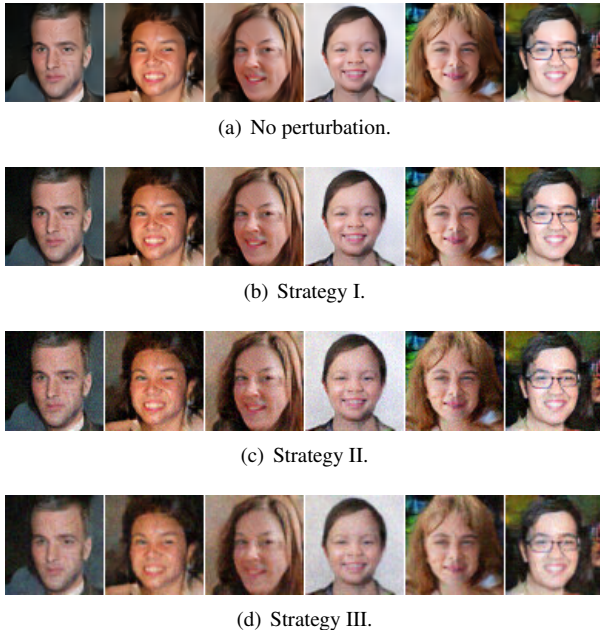


Figure 17: Adaptive attack II. From (a) strategy I to (c) strategy III, the magnitude of output perturbation gradually increases. The corresponding magnitudes are shown in Table 2. The average SSIM score for strategy I, strategy II, and strategy III is 92.20%, 82.97%, and 82.10%, respectively.

## A.6. Suspect Models

### A.6.1 Implementation details of suspect models

For positive suspect models, models from physical stealing (marked as PS) are the same as target models. We use model extraction attacks proposed in the work [13] to construct models from model extraction (marked as ME). Specifically, given  $m$  generated samples from a target model  $G_{tar}$ , the adversaries retrain a model (also called the substitute model or attack model) on  $m$  generated samples. Attack models can use any architecture, such as SNGAN, PGGAN, or StyleGAN. We study protection performance under model extraction attacks with different GANs as attack models in Section 6.4.

For negative suspect models, Ind-a is trained with the same architectures of target models but on dataset II. Ind-b is trained with the same architectures and datasets of target models but uses different seeds, i.e. different random initializations. Using different seeds means models trained on different training environments and optimization processes. Theoretically, models trained with different seeds should be different, because they do not derive from model extraction and physical stealing, and they are honest models with independent training. Thus, an ownership protection method should be able to differentiate them. Here, setups for negative suspect models are very similar to those for target models because we aim to test whether a protection method hurt honest model providers in the strong assumption setting. This requires that a protection method should be extremely robust.

### A.6.2 Performance of suspect models

In this section, we show the performance of suspect models. Overall, we choose suspect models with the best performance in each setting. For positive suspect models, that is these models which are obtained by physical stealing or model extraction attacks, we use  $FID(p_{\tilde{g}}, p_r)$  and  $FID(p_{\tilde{g}}, p_g)$  to demonstrate the performance. Here,  $p_{\tilde{g}}$  is the implicit distribution of a suspect model or an attack model.  $p_r$  is the implicit distribution of a training set.  $p_g$  is the implicit distribution of a target model.  $FID(p_{\tilde{g}}, p_g)$  repre-

Table 7: Performance of suspect positive models. The target model is SNGAN trained on FFHQ-I. It is corresponding to Figure 2.

| Types | Ong                       |                           | Yu                        |                           | Ours                      |                           |
|-------|---------------------------|---------------------------|---------------------------|---------------------------|---------------------------|---------------------------|
|       | Attack Performance        |                           | Attack Performance        |                           | Attack Performance        |                           |
|       | $FID(p_{\tilde{g}}, p_r)$ | $FID(p_{\tilde{g}}, p_g)$ | $FID(p_{\tilde{g}}, p_r)$ | $FID(p_{\tilde{g}}, p_g)$ | $FID(p_{\tilde{g}}, p_r)$ | $FID(p_{\tilde{g}}, p_g)$ |
| PS    | 20.14                     | 0.00                      | 26.46                     | 0.00                      | 20.25                     | 0.00                      |
| ME    | 25.47                     | 2.52                      | 30.83                     | 3.23                      | 27.60                     | 3.13                      |

Table 8: Performance of suspect negative models. The target model is SNGAN trained on FFHQ-I. FID( $p_r, p_g$ ) is used for evaluation.

| Types | Ong   | Yu    | Ours  |
|-------|-------|-------|-------|
| Ind-a | 17.84 | 17.84 | 17.84 |
| Ind-b | 20.63 | 29.13 | 17.15 |

Table 9: Performance of suspect positive models. The target model is SNGAN trained on FFHQ-I. It is corresponding to Figure 4.

| Attack Models | Ong                       |                           | Yu                        |                           |
|---------------|---------------------------|---------------------------|---------------------------|---------------------------|
|               | Attack Performance        |                           | Attack Performance        |                           |
|               | $FID(p_{\tilde{g}}, p_r)$ | $FID(p_{\tilde{g}}, p_g)$ | $FID(p_{\tilde{g}}, p_r)$ | $FID(p_{\tilde{g}}, p_g)$ |
| SNGAN         | 25.47                     | 2.52                      | 30.83                     | 3.23                      |
| PGGAN         | 23.58                     | 2.33                      | 29.29                     | 1.80                      |
| StyleGAN      | 21.62                     | 2.70                      | 27.27                     | 2.62                      |
| Ours          |                           |                           |                           |                           |
| SNGAN         | 27.60                     | 3.13                      |                           |                           |
| PGGAN         | 23.11                     | 2.56                      |                           |                           |
| StyleGAN      | 21.07                     | 2.97                      |                           |                           |

sents the similarity between an attack model and a target model, while  $FID(p_{\tilde{g}}, p_r)$  represents the similarity between an attack model and the training set of a target model. In the work [13], they are also called fidelity and accuracy, respectively. Here, we explicitly use  $FID(p_{\tilde{g}}, p_r)$  and  $FID(p_{\tilde{g}}, p_g)$  to report the performance of suspect positive models. For negative suspect models, we use  $FID(p_r, p_g)$  for evaluation.

Table 7 and Table 8 show positive and negative suspect models for target model SNGAN trained on FFHQ. Table 9 shows the performance of suspect positive models constructed by model extraction with different GANs. Table 10 and Table 11 show positive and negative suspect models for target model SNGAN trained on Church. Table 12 and Table 13 show positive and negative suspect models for target model StyleGAN trained on FFHQ.

Table 10: Performance of suspect positive models. The target model is SNGAN trained on Church-I. It is corresponding to Figure 9.

| Types | Attack Performance        |                           |
|-------|---------------------------|---------------------------|
|       | $FID(p_{\tilde{g}}, p_r)$ | $FID(p_{\tilde{g}}, p_g)$ |
| PS    | 12.96                     | 0.00                      |
| ME    | 19.17                     | 3.64                      |

Table 11: Performance of suspect negative models. The target model is SNGAN trained on Church-I.

| Types | $FID(p_r, p_g)$ |
|-------|-----------------|
| Ind-a | 13.35           |
| Ind-b | 14.56           |

Table 12: Performance of suspect positive models. The target model is StyleGAN trained on FFHQ-I. It is corresponding to Figure 15.

| Types | Attack Performance        |                           |
|-------|---------------------------|---------------------------|
|       | $FID(p_{\tilde{g}}, p_r)$ | $FID(p_{\tilde{g}}, p_g)$ |
| PS    | 8.76                      | 0.00                      |
| ME    | 12.61                     | 4.12                      |

Table 13: Performance of suspect negative models. The target model is StyleGAN trained on FFHQ-I.

| Types | $FID(p_r, p_g)$ |
|-------|-----------------|
| Ind-a | 17.84           |
| Ind-b | 8.92            |